Spectroscopic Analysis of Polymer and Monolayer MoS_2 Interfaces for Photodetection Applications

Christine K. McGinn,[1] Daniel M. Harrington,[1] Edwin Heilweil,[1] and Christina A. Hacker[1]
Physical Measurement Laboratory, National Institute of Standards and Technology, Gaithersburg, Maryland, USA

(*Electronic mail: christine.mcginn@nist.gov)

(Dated: 12 December 2023)

Polymer passivation has been leveraged to improve photodetection in two dimensional transition metal dichalcogenide field-effect transistors (2D TMD FETs). The relative passivation effects of common polymers, however, is not well understood. In this work, the interface of monolayer MoS_2 and three common polymers, Parylene N (Pa-N), polymethyl methacrylate (PMMA), and polyvinylidene difluoride trifluoroethylene (PVDF-TrFE), is assessed with multiple spectroscopic methods. Raman and photoluminescence spectroscopy demonstrate that Pa-N and PMMA provide an n doping effect, which increases photoconductivity and photogenerated charge in Terahertz domain and time-resolved spectroscopy. Terahertz time-resolved spectroscopy shows significantly longer carrier lifetime for MoS_2 coated with PVDF-TrFE compared to other polymers. These results suggest that PVDF-TrFE provides a unique benefit for photodetection applications.

Two-dimensional transition-metal dichalcogenides (2D TMDs) have been extensively studied for photodetection applications due to their strong optoelectronic behavior in the visible range and tunable band gap.[1] 2D TMD field effect transistors (FETs) have the advantage of large ON/OFF ratio and small form factor compared to other transistor based photodetectors.[2] However, the optoelectronic properties of 2D TMDs can deteriorate as a result of surface defects and exposure to air and water.[3,4] Researchers have used a variety of materials to combat this degradation and passivate the surface, most commonly hexagonal boron nitride.[5–7] Polymers are ideal for passivating 2D TMDs in photodetection applications as most are transparent in the visible range, and improvement in photodetection by polymer encapsulation has been previously shown.[8]

While the benefits of passivation are well understood, the relative passivation effect of different polymers has not been well defined despite significant study on the mechanisms of passivation.[9] Researchers in recent years have used polymers to perform significant modulation of the optoelectronic properties of hybrid devices via doping, passivation, dielectric screening, and capacitive effects.[10,11] These schemes illustrate that polymers can contribute multiple mechanisms to the polymer/2D TMD interface. In particular, the ferroelectric polymer polyvinylidene difluoride-trifluoroethylene (PVDF-TrFE) has been used to improve the bandwidth and responsivity of photodetectors in its poled state, but the other effects of the fluoropolymer's properties, including fluorinated structure, high dielectric constant, and even pyroelectricity, on the MoS_2 interface have not been studied in detail.[12,13] As the properties of 2D TMDs can be dramatically influenced by the surface condition, a careful assessment of the effects at the interface, including passivation, are needed to advance photodetector performance. In this work, the 2D TMD and polymer interface is assessed spectroscopically for three common polymers to evaluate the efficacy of each polymer in passivating the MoS_2 surface for photodetection applications. Evaluating this interface with spectroscopic methods, especially with dynamic pump probe measurements like time resolved THz spectroscopy, mimics the processes occurring during photodetection operation and thus provides a clearer understanding of the fundamental physics at play. Spectroscopic methods can provide significant qualitative and quantitative information about the chemical and electronic properties of the TMD monolayer. Terahertz spectroscopy has previously shown the ability to probe the conductivity and mobility of semiconductors without the need for contact.[14] As it can be difficult to establish good electrical contact with TMDs, this method is useful to remove any effects from the contact interface on carrier dynamics and electronic characterization.

For this study, a monolayer TMD was chosen rather than multilayer, even though it would provide less signal for many spectroscopic experiments, to simplify the carrier dynamics in the TMD so that the small changes anticipated from passivation could more easily be observed. In multilayer TMDs, the interlayer exciton overwhelms any other photogenerated carriers.[15] These interlayer excitons can be significantly longer lived than other carriers, further obfuscating the carrier dynamics. This study focuses on MoS_2 rather than another TMD because it is more air stable than other TMDs as some of the spectroscopic techniques required prolonged air exposure. To mitigate any degradation of the monolayer due to air exposure, the samples were stored in a nitrogen glovebox when not in use. A representative group of three commonly available polymers were chosen to understand the relative passivation effects: parylene N, polymethyl methacrylate (PMMA), and PVDF-TrFE. Parylene is an extremely inert polymer used frequently in organic electronics and biomedical devices for encapsulation that has previously been shown to passivate graphene.[16–18] Additionally, parylene is specifically engineered to act as a chemical barrier for water and other solvents, which is ideal to prevent degradation of the 2D TMD. The N formulation of parylene (Pa-N) was chosen for this study as it has almost no functional groups. PMMA is a standard electron beam photoresist frequently used to encapsulate 2D TMD devices for passivation and to prevent degradation.[19] PVDF-TrFE is an electroactive polymer that has been shown to be piezoelectric, pyroelectric, and ferroelectric, and as a

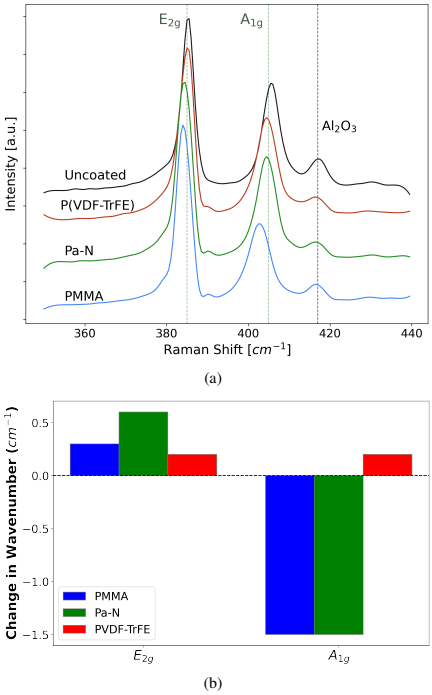

FIG. 1. a) Raman spectra of MoS_2 on sapphire with polymer coatings b) change in peak position from the same MoS_2 surface after polymer coating

result, is widely applied for flexible sensors.[20] PMMA and PVDF-TrFE have functional groups containing oxygen and fluorine that would be expected to better fix sulfur vacancies or provide doping than Pa-N. Pa-N also has the lowest dielectric constant of the three so should not provide much dielectric screening. This group of polymers then should provide reasonable insight into the mechanisms at the 2D TMD/polymer interface for photodetection applications.

CVD-grown monolayer MoS_2 was purchased from 2D Semiconductors and then approximately 300 nm of each polymer was deposited on top. PVDF-TrFE and PMMA were deposited by spin coating and Pa-N was deposited via physical vapor deposition. The PVDF-TrFE film was not poled so it does not contribute an electric field due to remnant polarization.

The samples were characterized before and after coating with Raman spectroscopy by using a 514 nm laser input. The resulting spectra after coating are shown in Fig. 1(a) and the change in peak positions as a result of coating is shown in Fig. 1(b). Raman spectroscopy was performed both before and after coating to account for any sample variation. No significant change in the location of Raman peaks was observed for samples coated with PVDF-TrFE, but for PMMA and Pa-N, a significant redshift was observed in the A_{1g} peak after coating. Previous work has shown that this shift can be attributed to n doping.[21–25] PMMA and Pa-N show a larger change than PVDF-TrFE, which reflects a higher doping level. This result suggests that previously shown device improvements as a result of PMMA or Pa-N encapsulation may have a doping contribution rather than a passivating one. This doping could be a result of the oxygen in PMMA's functional groups or stress on the film as a result of polymer deposition, but further investigation must be done to understand the exact mechanism.

Spatially-resolved photoluminescence (PL) spectra were collected by using a hyperspectral PL imaging microscope, where a full spectrum is collected for every pixel in an image. Spectra were collected over a 70 μm^2 area with a Photon etc. hyperspectral microscope using an incident 532 nm 26 mW excitation beam. In addition to areas with intense PL, there were visible grain boundaries and low-intensity spots on the MoS_2 films that we attribute to local variations in the precursor compounds used during the CVD growth.[26] In order to characterize just the MoS_2 film, we first divided the polymer sample spectra by the uncoated substrate control spectra to remove background noise, then masked the pixels with the lowest tenth percentile of intensity at the A exciton peak. The total collected area of $70\mu m^2$ consisted of 512×512 pixels, then removing the mask consisting of the lowest tenth percentile intensity pixels resulted in a final pixel count of 2.36×10^5, each with a full spectrum of PL intensities. The spectra were normalized based on the maximum of the A exciton peak at 670 nm. Pixels were binned and averaged to produce a distribution of PL spectra over the whole image area which is shown in Fig. 2(a).

The A exciton peak near 670 nm was not significantly changed as a result of PVDF-TrFE coating. For PMMA and Pa-N coating, the peak is redshifted as shown in the box plot in Fig. 2(b), which is consistent with the doping observed in the Raman spectra. Because the photoluminescence spectra is normalized to the A exciton peak, the B exciton at 625 nm is more prevalent for some samples than others. Additionally, the full width half maximum increases for the PMMA coating as shown in the box plot in Fig. 2(c), which is the opposite effect than what is usually expected for successful passivation.[27] These results suggest then that doping rather than passivation is the prominent mechanism at the interface.

To better understand changes in carrier generation, population, and dynamics as a result of polymer addition, time-resolved (photoexcitation or pump-probe) Terahertz spectroscopy (TRTS) was performed by sweeping the THz pump pulse optical delay with respect to the fixed THz probe. THz lock-in signals were acquired in step-scan delay mode and averaged. Detailed diagrams and descriptions of this technique have been previously published.[28,29] The spectroscopic setup is driven by a 1 kHz Ti:Sapphire 35 fs, 800 nm laser system that generates doubled 400 nm pump pulses to excite above the MoS_2 bandgap, employs a zinc telluride (ZnTe) crystal for THz probe pulse generation, and gating pulses for electro-optic ZnTe-based THz detection. The absorbance at 400 nm

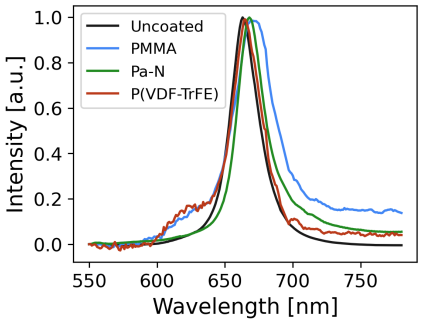

(a)

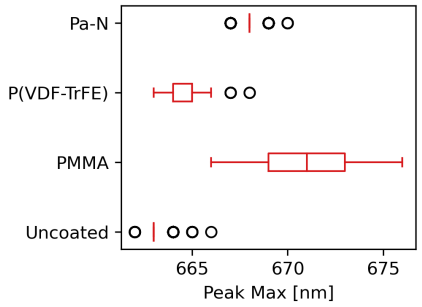

(b)

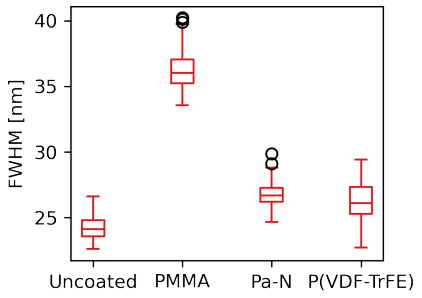

(c)

FIG. 2. Analysis of photoluminescence spectra taken via hyperspectral imaging a) normalized averaged spectra of MoS_2 on sapphire with polymer coatings b) box plot of A exciton peak location of spectra from hyperspectral microscope c) box plot of A exciton peak full width half maximum of spectra from hyperspectral microscope. While the boxes in b) and c) represent data at the 95% confidence level, the circles denote data outliers at the 50 % confidence interval.

of each sample was measured to ensure the polymer coatings did not significantly affect the 400 nm optical pump signal

TABLE I. Real and imaginary conductivity for monolayer MoS_2 with standard deviation

Coating	Real σ (S/cm)	Imaginary σ (S/cm)
None	37.81 ± 11.54	4.91 ± 1.31
PMMA	51.86 ± 5.01	-1.94 ± 0.59
Pa-N	66.16 ± 10.23	4.77 ± 2.74
PVDF-TrFE	40.16 ± 6.06	-8.59 ± 4.93

felt by the monolayer MoS_2. The absorbance of each sample was observed to be between 0.06 and 0.09, which agrees with literature values for MoS_2, indicating the polymers do not cause a significant change in absorbance. This technique also allows for the temporal mapping of the THz pulse electric field when using photoexcited and non-photoexcited conditions (Time-Domain Spectroscopy, TDS). The unpumped THz transmission $E_0(t)$ and differential pumped transmission $\Delta E(t, t_{pu})$, where t is the THz pump-probe delay and t_{pu} is the optical and THz pump delay, is Fourier-transformed to obtain the frequency-dependent complex-valued photoconductivity $\sigma(\omega, t_{pu})$:

$$\sigma(\omega, t_{pu}) = -\left(\frac{n_{THz}+1}{Z_0 d}\right)\frac{\Delta\widetilde{E}(\omega, t_{pu})}{\widetilde{E_0}(\omega)}, \qquad (1)$$

where n_{THz} is the index of refraction of the substrate, Z_0 is the free-space impedance, and d is the sample (e.g., monolayer MoS_2) thickness. The observed real and imaginary conductivity is shown in Fig. 3.[29]

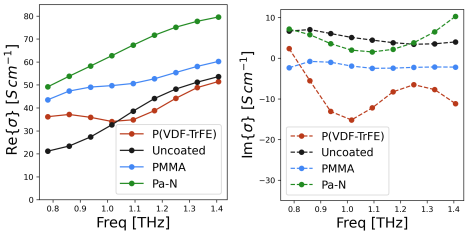

(a) (b)

FIG. 3. Optically measured a) real and b) imaginary conductivity for MoS_2 with polymers via time domain terahertz spectroscopy obtained at pump-probe maximum signal near zero time delay.

The real conductivity measured for all samples corresponds to those obtained in previous work for monolayer MoS_2.[30,31] Averaged values over the frequency range with associated standard deviation are shown in Table I.

The real conductivity of the samples coated with PVDF-TrFE and PMMA were within error of the uncoated sample. The Pa-N and PMMA coated samples show a higher real conductivity than the other measured samples, which corresponds to the n doping effect observed by Raman and photoluminescence spectroscopy. The difference in conductivity between

the Pa-N and PMMA sample could be accounted for by variations in the conductivity between the MoS_2 samples before coating as defects in the film can have a large impact on the conducitivty.

In TRTS spectra for each sample, we observed a sharp dip in THz transmission immediately following photoexcitation as shown in Fig. 4. In uncoated, Pa-N coated, and PMMA-coated samples, THz transmission recovered nearly to pre-excitation levels after around 5 ps, which is consistent with other reported values under similar conditions.[32,33] Secondary signals near 3 ps delay arise from substrate back reflections. The timing and amplitude of these reflections is dependent on step-scan delay position and substrate thickness which varies from sample to sample. These spurious signals are observed but do not contain any relevant information about carrier conductivity or population. The PVDF-TrFE sample retained a higher THz absorption out to a delay of 20 ps, which is indicative of the continued presence of charge carriers in the MoS_2 film.

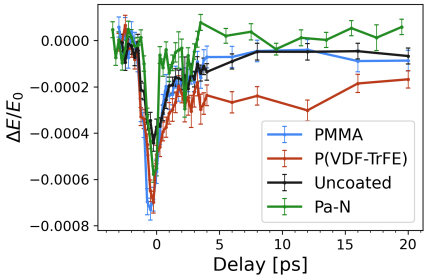

FIG. 4. Time-resolved terahertz spectroscopy response for MoS_2 on sapphire with polymer coatings.

The polymer coated samples all show more initial charge generation than the uncoated sample. This finding can be in part attributed to the doping effects shown in Raman and PL spectroscopy. The PVDF-TrFE coated sample has a significantly longer tail, which indicates a longer charge lifetime. There are several possible mechanisms that could be contributing to this result. The additional n doping from the Pa-N and PMMA coating causes an increased carrier concentration which can encourage the formation of lower mobility trions.[34] The fluorine content in the PVDF-TrFE could provide superior passivation of sulfur vacancies in the MoS_2 or draw out excess charge to limit recombination and trion formation.

This work assesses the relative passivation effects of common polymers on monolayer MoS_2 to identify what materials can be used to improve photodetection in 2D TMD FETs. While previous work cites the electric field arising from the remnant polarization of poled PVDF-TrFE is responsible for improved photodetection in 2D TMD FETs, this work suggests that the material properties of PVDF-TrFE contribute to the noted improvement in the carrier lifetimes of photogenerated charge.[12] These longer lifetimes will have a significant positive impact on the performance of an FET photodetector. While more work should be done to understand the exact mechanism at the PVDF-TrFE/2D TMD interface, this finding indicates that PVDF-TrFE and other fluoropolymers could be used to significantly improve photodetection in hybrid 2D TMD photodetectors. Future work will investigate if the findings in this work persist when these polymer coatings are added to multilayer TMDs, TMDs other than MoS_2, and TMD FETs.

ACKNOWLEDGMENTS

D.M.H. gratefully acknowledges support from the NIST Summer Undergraduate Research Fellowship. C.K.M. gratefully acknowledges funding from the National Research Council Research Associateship Program. The authors gratefully acknowledge Adam Biacchi for assistance and training on the use of the Raman spectrometer and hyperspectral imaging microscope.

DATA AVAILABILITY STATEMENT

The data that support the findings of this study are available from the corresponding author upon reasonable request.

CONFLICT OF INTEREST

The data that support the findings of this study are available from the corresponding author upon reasonable request.

ADDITIONAL INFORMATION

The full description of the procedures used in this paper requires the identification of certain commercial products. The inclusion of such information should in no way be construed as indicating that such products are endorsed by the National Institute of Standards and Technology, or are recommended by the National Institute of Standards and Technology, or that they are necessarily the best materials for the purposes described.

[1]H. S. Nalwa, "A review of molybdenum disulfide (mos2) based photodetectors: From ultra-broadband, self-powered to flexible devices," RSC Advances **10**, 30529–30602 (2020).
[2]C. C. Wu, D. Jariwala, V. K. Sangwan, T. J. Marks, M. C. Hersam, and L. J. Lauhon, "Elucidating the photoresponse of ultrathin mos2 field-effect transistors by scanning photocurrent microscopy," Journal of Physical Chemistry Letters **4**, 2508–2513 (2013).
[3]D. J. Late, B. Liu, H. R. Matte, V. P. Dravid, and C. Rao, "Hysteresis in single-layer mos2 field effect transistors," ACS nano **6**, 5635–5641 (2012).
[4]W. Park, J. Park, J. Jang, H. Lee, H. Jeong, K. Cho, S. Hong, and T. Lee, "Oxygen environmental and passivation effects on molybdenum disulfide field effect transistors," Nanotechnology **24**, 095202 (2013).
[5]K. Zhang, Y. Feng, F. Wang, Z. Yang, and J. Wang, "Two dimensional hexagonal boron nitride (2d-hbn): Synthesis, properties and applications," (2017).

[6]B. Sirota, N. Glavin, S. Krylyuk, A. V. Davydov, and A. A. Voevodin, "Hexagonal mote2 with amorphous bn passivation layer for improved oxidation resistance and endurance of 2d field effect transistors," Scientific Reports **8**, 8668 (2018).
[7]D. Wu, J. Guo, C. Wang, X. Ren, Y. Chen, P. Lin, L. Zeng, Z. Shi, X. J. Li, C.-X. Shan, *et al.*, "Ultrabroadband and high-detectivity photodetector based on ws2/ge heterojunction through defect engineering and interface passivation," ACS nano **15**, 10119–10129 (2021).
[8]J. Ma, K.-Y. Choi, S. H. Kim, H. Lee, and G. Yoo, "All polymer encapsulated, highly-sensitive mos2 phototransistors on flexible par substrate," Applied Physics Letters **113** (2018).
[9]Z. Hu, Z. Wu, C. Han, J. He, Z. Ni, and W. Chen, "Two-dimensional transition metal dichalcogenides: interface and defect engineering," Chem. Soc. Rev. **47**, 3100–3128 (2018).
[10]K. Cho, J. Pak, S. Chung, and T. Lee, "Recent advances in interface engineering of transition-metal dichalcogenides with organic molecules and polymers," ACS Nano **13**, 9713–9734 (2019).
[11]J. Ji and J. H. Choi, "Recent progress in 2d hybrid heterostructures from transition metal dichalcogenides and organic layers: properties and applications in energy and optoelectronics fields," (2022).
[12]X. Wang, P. Wang, J. Wang, W. Hu, X. Zhou, N. Guo, H. Huang, S. Sun, H. Shen, T. Lin, M. Tang, L. Liao, A. Jiang, J. Sun, X. Meng, X. Chen, W. Lu, and J. Chu, "Ultrasensitive and broadband mos2 photodetector driven by ferroelectrics," Advanced Materials **27**, 6575–6581 (2015).
[13]S. Zhu, D. Li, Q. Wang, Z. He, Y. Wu, H. Lin, L. B. Huang, H. Huang, S. Gao, J. Wang, Z. Gong, Q. Qin, and X. Wang, "Exciton emissions in bilayer wse2tuned by the ferroelectric polymer," Journal of Physical Chemistry Letters **13**, 1636–1643 (2022).
[14]B. G. Alberding, W. R. Thurber, and E. J. Heilweil, "Direct comparison of time-resolved terahertz spectroscopy and hall van der pauw methods for measurement of carrier conductivity and mobility in bulk semiconductors," J. Opt. Soc. Am. B **34**, 1392–1406 (2017).
[15]T. Mueller and E. Malic, "Exciton physics and device application of two-dimensional transition metal dichalcogenide semiconductors," (2018).
[16]S. Gholizadeh, D. M. Lincoln, Z. Allahyari, L. P. Widom, R. N. Carter, and T. R. Gaborski, "Optimization of parylene c and parylene n thin films for use in cellular co-culture and tissue barrier models," Scientific Reports **13**, 4262 (2023).
[17]H. Park, H. Ahn, J. Kwon, S. Kim, and S. Jung, "Parylene-based double-layer gate dielectrics for organic field-effect transistors," ACS applied materials & interfaces **10**, 37767–37772 (2018).
[18]A. F. Rigosi, C.-I. Liu, B. Y. Wu, H.-Y. Lee, M. Kruskopf, Y. Yang, H. M. Hill, J. Hu, E. G. Bittle, J. Obrzut, A. R. Hight Walker, R. E. Elmquist, and D. B. Newell, "Examining epitaxial graphene surface conductivity and quantum hall device stability with parylene passivation," Microelectronic Engineering **194**, 51–55 (2018).
[19]U. Ali, K. J. B. A. Karim, and N. A. Buang, "A review of the properties and applications of poly (methyl methacrylate)(pmma)," Polymer Reviews **55**, 678–705 (2015).
[20]B. Stadlober, M. Zirkl, and M. Irimia-Vladu, "Route towards sustainable smart sensors: Ferroelectric polyvinylidene fluoride-based materials and their integration in flexible electronics," Chemical Society Reviews **48**, 1787–1825 (2019).
[21]S. Zhang, H. M. Hill, K. Moudgil, C. A. Richter, A. R. H. Walker, S. Barlow, S. R. Marder, C. A. Hacker, and S. J. Pookpanratana, "Controllable, wide-ranging n-doping and p-doping of monolayer group 6 transition-metal disulfides and diselenides," Advanced Materials **30** (2018), 10.1002/adma.201802991.
[22]M. Tebyetekerwa, J. Zhang, Z. Xu, T. N. Truong, Z. Yin, Y. Lu, S. Ramakrishna, D. Macdonald, and H. T. Nguyen, "Mechanisms and applications of steady-state photoluminescence spectroscopy in two-dimensional transition-metal dichalcogenides," ACS nano **14**, 14579–14604 (2020).
[23]G. Kukucska and J. Koltai, "Theoretical investigation of strain and doping on the raman spectra of monolayer mos2," Physica Status Solidi (B) Basic Research **254** (2017), 10.1002/pssb.201700184.
[24]B. Chakraborty, A. Bera, D. V. Muthu, S. Bhowmick, U. V. Waghmare, and A. K. Sood, "Symmetry-dependent phonon renormalization in monolayer mos 2 transistor," Physical Review B - Condensed Matter and Materials Physics **85** (2012), 10.1103/PhysRevB.85.161403.
[25]B. Liu, W. Zhao, Z. Ding, I. Verzhbitskiy, L. Li, J. Lu, J. Chen, G. Eda, and K. P. Loh, "Engineering bandgaps of monolayer mos2and ws2on fluoropolymer substrates by electrostatically tuned many-body effects," Advanced Materials **28**, 6457–6464 (2016).
[26]I. S. Kim, V. K. Sangwan, D. Jariwala, J. D. Wood, S. Park, K.-S. Chen, F. Shi, F. Ruiz-Zepeda, A. Ponce, M. Jose-Yacaman, V. P. Dravid, T. J. Marks, M. C. Hersam, and L. J. Lauhon, "Influence of stoichiometry on the optical and electrical properties of chemical vapor deposition derived mos2," ACS Nano **8**, 10551–10558 (2014).
[27]Q. Cui, Z. Luo, Q. Cui, W. Zhu, H. Shou, C. Wu, Z. Liu, Y. Lin, P. Zhang, S. Wei, H. Yang, S. Chen, A. Pan, and L. Song, "Robust and high photoluminescence in ws2 monolayer through in situ defect engineering," Advanced Functional Materials **31** (2021), 10.1002/adfm.202105339.
[28]M. C. Beard, G. M. Turner, and C. A. Schmuttenmaer, "Terahertz spectroscopy," J. Phys. Chem. B **106**, 7146—-7159 (2002).
[29]B. G. Alberding, A. J. Biacchi, A. R. H. Walker, and E. J. Heilweil, "Charge carrier dynamics and mobility determined by time-resolved terahertz spectroscopy on films of nano-to-micrometer-sized colloidal tin(ii) monosulfide," J. Phys. Chem. C **120**, 15395—-15406 (2016).
[30]C. J. Docherty, P. Parkinson, H. J. Joyce, M.-H. Chiu, C.-H. Chen, M.-Y. Lee, L.-J. Li, L. M. Herz, and M. B. Johnston, ACS Nano **8**, 11147–11153 (2014).
[31]H. Gao, J. Suh, M. C. Cao, A. Y. Joe, F. Mujid, K.-H. Lee, S. Xie, P. Poddar, J.-U. Lee, K. Kang, P. Kim, D. A. Muller, and J. Park, "Tuning electrical conductance of mos2 monolayers through substitutional doping," Nano Letters **20**, 4095–4101 (2020).
[32]X. Xing, L. Zhao, Z. Zhang, X. Lin1, Y. Yu, Z. Jin, W. Liu, W. Zhang, and G. Ma, "The modulation of terahertz photoconductivity in cvd grown n-doped monolayer mos2 with gas adsorption," Journal of Physics: Condensed Matter **31**, 245001 (2019).
[33]J. K. Gustafson, D. Wines, E. Gulian, C. Ataca, and L. M. Hayden, "Positive and negative photoconductivity in monolayer mos2 as a function of physisorbed oxygen," J. Phys. Chem. C **125**, 8712—-8718 (2021).
[34]C. Lui, A. Frenzel, D. Pilon, Y.-H. Lee, X. Ling, G. Akselrod, J. Kong, and N. Gedik, "Trion-induced negative photoconductivity in monolayer mos 2," Physical review letters **113**, 166801 (2014).
[35]X. Liu and M. C. Hersam, "Interface characterization and control of 2d materials and heterostructures," Advanced Materials **30**, 1–34 (2018).
[36]C. J. Docherty, P. Parkinson, H. J. Joyce, M.-H. Chiu, C.-H. Chen, M.-Y. Lee, L.-J. Li, L. M. Herz, and M. B. Johnston, "Ultrafast transient terahertz conductivity of monolayer mos2 and wse2 grown by chemical vapor deposition," ACS nano **8**, 11147–11153 (2014).